Appl. Phys. B 89, 91–97 (2007)
DOI: 10.1007/s00340-007-2763-y

Applied Physics B
Lasers and Optics

H.T. EYYUBOĞLU[1,✉]
Y. BAYKAL[1]
Y. CAI[2]

Degree of polarization for partially coherent general beams in turbulent atmosphere

[1] Department of Electronic and Communication Engineering, Çankaya University, Öğretmenler Cad. No. 14 Yüzüncüyıl, 06530 Balgat, Ankara, Turkey
[2] Max-Planck-Research-Group, Institute of Optics, Information and Photonics, University of Erlangen, Staudtstr. 7/B2, 91058, Erlangen, Germany

Received: 8 June 2007/Revised version: 31 July 2007
Published online: 31 August 2007 •

ABSTRACT The degree of polarization is found for optical excitations of cosh-Gaussian, cos-Gaussian and annular-Gaussian beams in a turbulent atmosphere. The related formulation is based on the beam coherence polarization matrix. The self and mutual coherence functions appearing in the beam coherence polarization matrix are evaluated, when the above mentioned excitations exhibit partial source coherence for self and cross fields. Plots showing the variation of the degree of polarization are provided versus the propagation length when the source size, displacement parameter, structure constant and the degree of source coherence for self and cross fields change.

PACS 42.25.Dd; 42.25.Ja; 42.25.Kb

1 Introduction

Polarization changes of beams along the propagation axis have recently been the subject of many articles. In this context, Gori gave a matrix treatment for partially polarized and partially coherent beams proposing the name beam coherence polarization (BPC) matrix [1]. Piquero et al. devised an experimental setup based on a Mach–Zehnder interferometer for the synthesis of partially polarized Gaussian Schell-model (GSM) sources [2]. In another study [3], by taking the argument of the Laguerre part as complex, Deng et al. analysed the propagation of radially polarized elegant light beams. Duan and Lü reported on the polarization properties of Gaussian beams in the far field using the nonparaxial approach [4]. For GSM beams, Gori et al. derived the degree of polarization expression giving examples of how the degree of polarization is affected as the beam progresses along the propagation axis [5]. With the help of the tensor method, Cai and his co-workers conducted a study on the properties of partially coherent and partially polarized beams for the fractional Fourier transform plane [6]. Through the use of cross spectral density functions, propagation induced polarization changes for partially coherent Gaussian beams were investigated by Agrawal and Wolf [7]. For stochastic electromagnetic beams, it was shown in a recent article by Pu and others that the spectra of the radiated field depend both on coherence properties of the source and its degree of polarization and also appear differently in different directions of observation [8].

The above mentioned works mostly concern propagation in free space. There are also studies carried out for other types of propagation media. Among these, the following may be cited. Wolf provided a unified formalism of coherence and polarization dealing with the determination of degree of polarization changes as the beam propagates in free space and random media [9]. Ge et al. examined the propagation of partially polarized GSM beams in dispersive and absorbing media [10]. By adopting Tatarskii model of the power spectrum, Roychowdhury and others performed a study on the polarization changes of partially coherent sources in atmospheric turbulence [11]. The far field degree of polarization behaviour of partially coherent beams propagating in turbulent conditions was considered, formulated and evaluated by Korotkova et al. [12]. Recently, Ji, Zhang and Lü studied the polarization of polychromatic partially coherent beams in a turbulent atmosphere [13]. Within the context of laser beam shaping applications, Shealy and Hoffnagle reported [14] a general comparison of four flattened beams, namely the super-Gaussian, flattened Gaussian, Fermi–Dirac, and super-Lorentzian.

It is well known [15] that the coherence and polarization are two important characteristics of laser beams which have a strong influence on the intensity and spectrum properties of the beams. The importance of the polarization of a beam in a turbulent atmosphere is that polarization can affect the behaviour of performance parameters in an atmospheric optical communications link. For example, it is shown by Korotkova [16] that partial polarization can be used, together with partial coherence, to reduce the scintillation index. It is also known [11] that when a Gaussian Schell-model source beam propagates in a turbulent atmosphere, the degree of polarization at the receiver plane first varies but after propagating a sufficiently long distance, the degree of polarization at the receiver plane attains the same value as that of the degree of polarization at the source plane.

The studies on the degree of polarization changes during propagation of optical beams have so far been mainly confined to source beams of Gaussian profile. Our aim in this article is to extend such analysis to other beam types, namely

✉ Fax: +90-312-284-8043, E-mail: h.eyyuboglu@cankaya.edu.tr

to cosh-Gaussian, cos-Gaussian and annular-Gaussian beams, with the aid of generalized beam formulation that we introduced some time ago [17]. For such an undertaking, we are motivated by the fact that the selection of the right kind of incident beam is an essential part of obtaining favourable beam characteristics on the receiver plane.

In some of our recent works [18, 19], we have found that cosh and cos-Gaussian beams in comparison with the fundamental Gaussian beam, offer favourable scintillation characteristics at certain propagation ranges, which can be an important criteria in atmospheric optical communications link design. Therefore, it becomes essential to investigate other beam types. Among the above cited studies, several applications of radially polarized laser beams are mentioned in [3]. Some of these are particle guiding, acceleration, scanning optical microscopy, determination of fluorescent molecule orientation and laser cutting. In communication, polarization properties can be utilized for diversity and multiplexing operations. For this purpose polarization filters can be placed in front of conventional detectors in order to separate x and y polarized fields. It is extracted from [14] that when the parameters of beam profiles from each family of distributions are constrained so that each profile has an equal radius and slope at half-maximum irradiance, then both near and far-field diffraction patterns can not be distinguished reasonably using common detectors. The difficulty experienced by such detectors to differentiate between different beam profiles as reported in [14] may still remain also in the case of partially polarized beams even when polarization filters are used.

2 Formulation

The x and y polarized field components of a lowest order coherent generalized beam, comprising a summation over N beams, can be written as [17]

$$\begin{aligned} u_{\mathrm{x}}(\boldsymbol{s}) &= u_{\mathrm{x}}(s_x, s_y) \\ &= \sum_{\ell=1}^{N} A_{\mathrm{x}\ell} \exp(-j\theta_{\mathrm{x}\ell}) \exp\left[-k\alpha_{\mathrm{x}\ell}\left(s_x^2+s_y^2\right)\right] \\ &\qquad \times \exp[-jV_{\mathrm{x}\ell}(s_x+s_y)]\,, \end{aligned} \tag{1}$$

$$\begin{aligned} u_{\mathrm{y}}(\boldsymbol{s}) &= u_{\mathrm{y}}(s_x, s_y) \\ &= \sum_{\ell=1}^{N} A_{\mathrm{y}\ell} \exp(-j\theta_{\mathrm{y}\ell}) \exp\left[-k\alpha_{\mathrm{y}\ell}\left(s_x^2+s_y^2\right)\right] \\ &\qquad \times \exp[-jV_{\mathrm{y}\ell}(s_x+s_y)]\,, \end{aligned} \tag{2}$$

where $\boldsymbol{s}$ is the transverse source plane vector and (s_x, s_y) stands for the decomposition of $\boldsymbol{s}$ into x and y directions. $A_{\mathrm{x}\ell}$ and $\theta_{\mathrm{x}\ell}$ denote respectively the amplitude and the phase of the ℓth component of the source field for the x polarized field. $\alpha_{\mathrm{x}\ell} = 1/(k\alpha_{\mathrm{xs}\ell}^2) + 0.5j/F_{\mathrm{x}\ell}$, thus $\alpha_{\mathrm{xs}\ell}$ and $F_{\mathrm{x}\ell}$ are Gaussian radial source size and the source focusing parameter, $k = 2\pi/\lambda$ is the wave number with λ being the wavelength and $j = (-1)^{0.5}$. $V_{\mathrm{x}\ell}$ is the complex displacement parameter giving rise to cosh-Gaussian and cos-Gaussian beams. Identical definitions apply for the y polarized field.

Equations (1) and (2) represent the deterministic parts of the source fields. To introduce partial coherence originating from random phase shift and tilt, we employ the formalism reported in our earlier work [20]. With this adoption, the degree of coherence for the x polarized field with itself becomes ϱ_{xx}. Similarly ϱ_{yy} will refer to the degree of self coherence for the y polarized field. The parameters, $\varrho_{\mathrm{xy}} = \varrho_{\mathrm{yx}}$, will, in the mean time, measure the degree of cross coherence between x and y polarized fields.

After furnishing the source beam with this partial coherence property, mutual coherence functions for the x and y polarized fields and their cross-products can be stated as

$$\Gamma_{\mathrm{qr}}(\boldsymbol{s}_1, \boldsymbol{s}_2) = u_{\mathrm{q}}(\boldsymbol{s}_1) u_{\mathrm{r}}^*(\boldsymbol{s}_2) \exp\left[-0.25(\boldsymbol{s}_1-\boldsymbol{s}_2)^2/\varrho_{\mathrm{qr}}^2\right]. \tag{3}$$

Here similar notation as in [1, 4, 12] is used, where $\mathrm{q} = \mathrm{x}, \mathrm{y}$ and $\mathrm{r} = \mathrm{x}, \mathrm{y}$ and $*$ denotes the conjugate. $\boldsymbol{s}_1$ and $\boldsymbol{s}_2$ are two distinct locations of the source plane. ϱ_{qr} represents the degree of source coherence for self and cross fields.

In a turbulent propagation medium, for obtaining the mutual coherence functions evaluated at the same (a single) point $\boldsymbol{p} = (p_x, p_y)$ on a receiver plane located at an axial distance of L away from the source plane, we utilize the extended Huygens–Fresnel principle in the following manner [13]

$$\begin{aligned} \Gamma_{\mathrm{qr}}(\boldsymbol{p}, \boldsymbol{p}, L) = b^2 \int_{-\infty}^{\infty}\int_{-\infty}^{\infty} & \mathrm{d}^2\boldsymbol{s}_1\, \mathrm{d}^2\boldsymbol{s}_2\, \Gamma_{\mathrm{qr}}(\boldsymbol{s}_1, \boldsymbol{s}_2) \\ & \times \exp\left[jb\left(|\boldsymbol{p}-\boldsymbol{s}_1|^2 - |\boldsymbol{p}-\boldsymbol{s}_2|^2\right)\right] \\ & \times \exp\left(-|\boldsymbol{s}_1-\boldsymbol{s}_2|^2/\varrho_0^2\right), \end{aligned} \tag{4}$$

where, $b = 0.5k/L$, the symbol $|\cdot|$ means the absolute value, $\varrho_0 = (0.545 C_n^2 k^2 L)^{-3/5}$ indicates the coherence length of a spherical wave propagating in the turbulent medium and C_n^2 is structure constant.

By the use of (3.462.2) of [21], the integration in (4) can be performed to arrive at the following analytic expression.

$$\begin{aligned} \Gamma_{\mathrm{qr}}(\boldsymbol{p}, \boldsymbol{p}, L) = b^2 \varrho_{\mathrm{qr}}^2 \varrho_0^2 \sum_{\ell_1=1}^{N}\sum_{\ell_2=1}^{N} & A_{\mathrm{q}\ell_1} A_{\mathrm{r}\ell_2}^* \exp[-j(\theta_{\mathrm{q}\ell_1} - \theta_{\mathrm{r}\ell_2})] \\ & \times \frac{X_{\mathrm{qr}x} X_{\mathrm{qr}y}}{T_{\mathrm{qr}}}\,. \end{aligned} \tag{5}$$

It is known that the mutual coherence function, $\Gamma_{\mathrm{qr}}(\boldsymbol{p}, \boldsymbol{p}, L)$ of (5) has to satisfy the non-negativity condition mentioned in [5]. In our case since the two coordinates of the transverse plane are taken the same, such requirement is already fulfilled. The definitions of various terms appearing in (5) are given below.

$$X_{\mathrm{qr}x} = \exp\left[-\frac{\varrho_{\mathrm{qr}}^2\varrho_0^2 T_{\mathrm{qr}x}(2bp_x - V_{\mathrm{q}\ell_1})^2 + Q_{\mathrm{qr}x}^2}{4\left(k\alpha_{\mathrm{q}\ell_1}\varrho_{\mathrm{qr}}^2\varrho_0^2 + \varrho_{\mathrm{qr}}^2 + 0.25\varrho_0^2 - jb\varrho_{\mathrm{qr}}^2\varrho_0^2\right)T_{\mathrm{qr}}}\right], \tag{6}$$

$$\begin{aligned} T_{\mathrm{qr}} &= k^2\alpha_{\mathrm{q}\ell_1}\alpha_{\mathrm{r}\ell_2}^*\varrho_{\mathrm{qr}}^2\varrho_0^2 + k\left(\alpha_{\mathrm{q}\ell_1} + \alpha_{\mathrm{r}\ell_2}^*\right)\left(\varrho_{\mathrm{qr}}^2 + 0.25\varrho_0^2\right) \\ &\quad + jkb\varrho_{\mathrm{qr}}^2\varrho_0^2\left(\alpha_{\mathrm{q}\ell_1} - \alpha_{\mathrm{r}\ell_2}^*\right) + b^2\varrho_{\mathrm{qr}}^2\varrho_0^2\,, \end{aligned} \tag{7}$$

$$\begin{aligned} Q_{\mathrm{qr}x} &= 2b\varrho_{\mathrm{qr}}^2\varrho_0^2(k\alpha_{\mathrm{q}\ell_1} - jb)p_x \\ &\quad + V_{\mathrm{r}\ell_2}^*\left(k\alpha_{\mathrm{q}\ell_1}\varrho_{\mathrm{qr}}^2\varrho_0^2 + \varrho_{\mathrm{qr}}^2 + 0.25\varrho_0^2 - jb\varrho_{\mathrm{qr}}^2\varrho_0^2\right) \\ &\quad - V_{\mathrm{q}\ell_1}\left(\varrho_{\mathrm{qr}}^2 + 0.25\varrho_0^2\right). \end{aligned} \tag{8}$$

From (6) and (8), X_{qry} and Q_{qry} are found simply by replacing p_x with p_y.

The beam coherence polarization (abbreviated as BCP) matrix can be stated as [1, 2, 5, 6, 10, 11]

$$P(\boldsymbol{p}, L) = \begin{pmatrix} \Gamma_{xx}(\boldsymbol{p}, \boldsymbol{p}, L) & B_{xy}\Gamma_{xy}(\boldsymbol{p}, \boldsymbol{p}, L) \\ B_{yx}\Gamma_{yx}(\boldsymbol{p}, \boldsymbol{p}, L) & \Gamma_{yy}(\boldsymbol{p}, \boldsymbol{p}, L) \end{pmatrix}, \quad (9)$$

where B_{xy} and B_{yx} with the restrictions of $B_{xy} = B^*_{yx}$ and $|B_{xy}| \leq 1$ are the distance independent cross correlation coefficients between the x and y polarized fields. In (9), the matrix elements, i.e., $\Gamma_{xx}(\boldsymbol{p}, \boldsymbol{p}, L)$, $\Gamma_{xy}(\boldsymbol{p}, \boldsymbol{p}, L)$, $\Gamma_{yx}(\boldsymbol{p}, \boldsymbol{p}, L)$ and $\Gamma_{yy}(\boldsymbol{p}, \boldsymbol{p}, L)$ can be retrieved from (5) by successively setting q = x, y and r = x, y.

Finally, the degree of polarization at a transverse coordinate, $\boldsymbol{p}$ on a receiver plane that is a distance L away from the source plane is defined to be [1, 2, 5, 6, 10, 11]

$$\gamma(\boldsymbol{p}, L) = (1 - 4\det[P(\boldsymbol{p}, L)]/\{\mathrm{Tr}[P(\boldsymbol{p}, L)]\}^2)^{0.5}\,. \quad (10)$$

Here, the operators Det and Tr respectively correspond to taking the determinant and trace of $P(\boldsymbol{p}, L)$ as given by (9).

3 Results and discussions

In this section, discussions and graphical illustrations are offered based on the numerical evaluation of (10) for cosh-Gaussian, cos-Gaussian, Gaussian and annular-Gaussian beams. These specific beams are generated from (1) and (2), by selecting the source parameters as listed in Table 1 of [22]. In this study however, for annular-Gaussian beams, it is to be noted that the amplitude coefficient of the secondary beam is 0.9 of the primary beam, and the source size of the secondary beam is 0.8 of the primary beam.

Our graphical outputs employ a single wavelength of operation, which is $\lambda = 1.55\ \mu$m. Collimated beams are used, hence $F_x = F_y \to \infty$. All throughout the illustrations, the cross correlation coefficients of B_{xy} and B_{yx} are uniformly set to 0.4 and the degree of polarization is evaluated at on-axis, which means that $\boldsymbol{p}$ is equated to zero in (10). As a result, legend boxes in our figures, do not contain such common information.

Initially, by arranging the source and propagation parameters as shown in the figure, Fig. 1 displays the progress of six beam types along the propagation axis starting from the vicinity of source plane, up to a propagation length of $L = 10^8$ m. Here cosh-Gaussian and cos-Gaussian beams are taken twice, once with equal displacements for x and y polarizations, in the other instance, V_x and V_y are taken to have different magnitudes. From Fig. 1, it is observed that if the only difference between the x and y polarized source beams lies in their partial coherence parameters as in the case of cosh-Gaussian, cos-Gaussian beams having equal displacement parameters, and

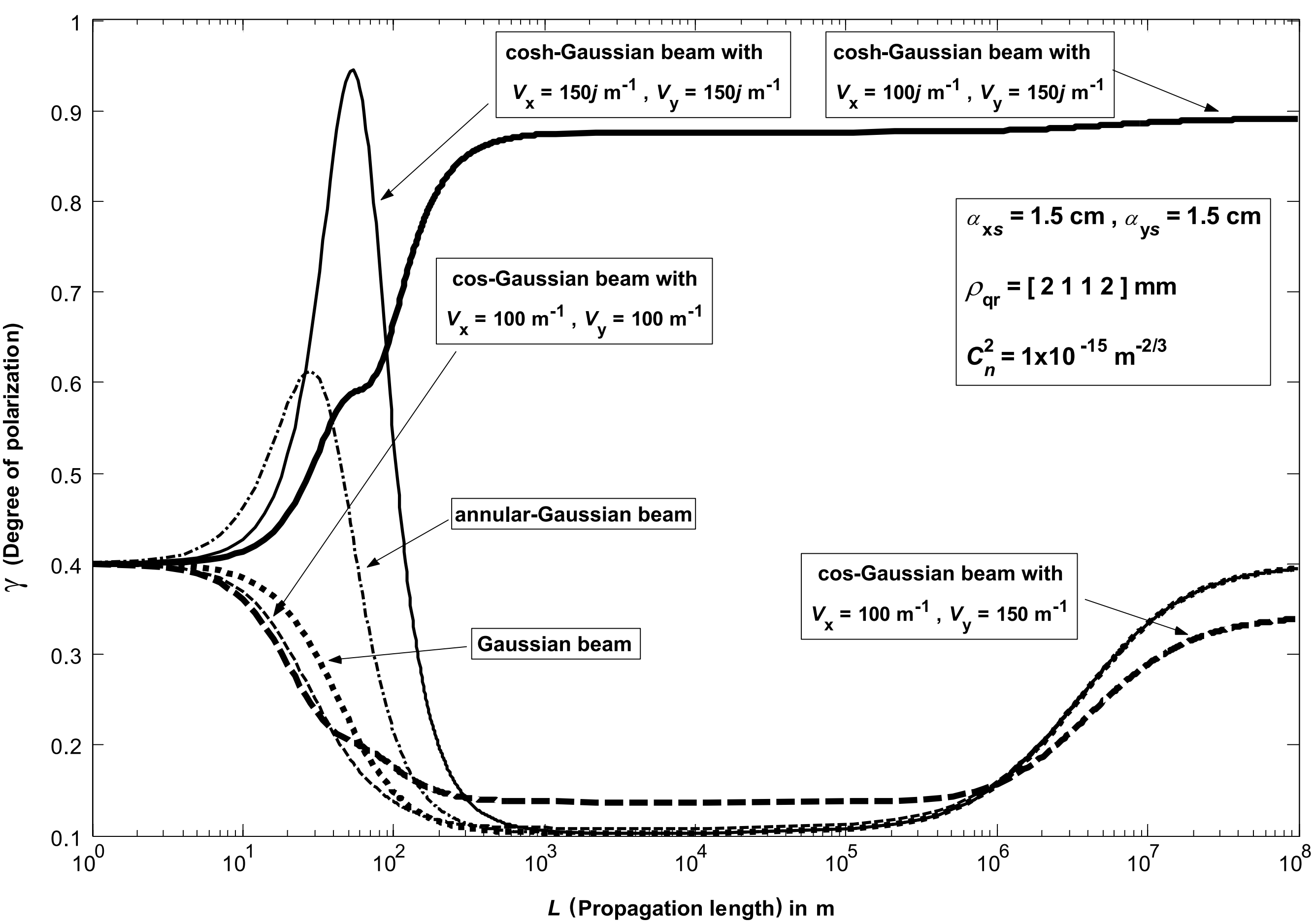

FIGURE 1 Variation of degree of polarization versus propagation length for six beam types

Gaussian and annular-Gaussian beams, then the degree of polarization is maintained at the value of 0.4 for a short distance further from the source plane. But as the propagation length is extended, a drop is experienced. Eventually at excessive propagation lengths, degree of polarization returns to the original value of 0.4. However, a cosh-Gaussian beam with unequal displacement parameters demonstrates nearly the opposite behaviour, that is, with advance of propagation distance, the degree of polarization gradually rises towards unity after a step rise occurring in the short propagation range. The cos-Gaussian beam possessing unequal displacement parameters exhibits a behaviour analogous to pure Gaussian and cos-Gaussian of equal displacement, but in the end, the degree of polarization for cos-Gaussian beam falls somewhere below the limiting value of 0.4. Cosh-Gaussian beams of equal displacement parameters and annular beam are characterized by humps at earlier propagation distances, while in the rest of the propagation range, they follow the same trend as the majority of the beams in Fig. 1.

To better understand the phenomena encountered in Fig. 1, we take the simple case of a Gaussian beam and assume that for x and y polarizations, all the beam parameters are identical except the coherence parameter settings of $\varrho_{qr} = [\varrho_{xx}\ \varrho_{xy}\ \varrho_{xy}\ \varrho_{xx}]$. In these circumstances, the mutual coherence functions in the matrix elements of (9) become diagonally equivalent, that is, $\Gamma_{xx}(\boldsymbol{p},\boldsymbol{p},L) = \Gamma_{yy}(\boldsymbol{p},\boldsymbol{p},L)$ and $\Gamma_{xy}(\boldsymbol{p},\boldsymbol{p},L) = \Gamma_{yx}(\boldsymbol{p},\boldsymbol{p},L)$. This way, the degree of polarization as defined by (10) will transform into

$$\begin{aligned}
&\gamma(\boldsymbol{p}=0,L)\\
&= |B_{xy}|\Gamma_{xy}(\boldsymbol{p}=0,\boldsymbol{p}=0,L)/\Gamma_{xx}(\boldsymbol{p}=0,\boldsymbol{p}=0,L)\\
&= |B_{xy}|\\
&\quad\times\frac{\varrho_{xy}^2\left(k^2\alpha_{xs}^4\varrho_{xx}^2\varrho_0^2 + 8\alpha_{xs}^2L^2\varrho_{xx}^2 + 2\alpha_{xs}^2\varrho_0^2L^2 + 4\varrho_{xx}^2\varrho_0^2L^2\right)}{\varrho_{xx}^2\left(k^2\alpha_{xs}^4\varrho_{xy}^2\varrho_0^2 + 8\alpha_{xs}^2L^2\varrho_{xy}^2 + 2\alpha_{xs}^2\varrho_0^2L^2 + 4\varrho_{xy}^2\varrho_0^2L^2\right)}\,.
\end{aligned} \tag{11}$$

In writing for (11), the exponential terms, X_{qrx} and X_{qry} are taken as unity, since we are operating on axis, i.e., $\boldsymbol{p} = 0$.

It is clear from (11) that as L approaches zero or as L gets very large, the degree of polarization approximates to $\gamma(\boldsymbol{p}=0,L) \to |B_{xy}|$. Meanwhile for most of the propagation lengths in-between, the term, $2\alpha_{xs}^2\varrho_0^2L^2$, present both in the numerator and denominator of the fourth line of (11) will dominate, hence in this region, degree of polarization will roughly reduce to $\gamma(\boldsymbol{p}=0,L) \simeq |B_{xy}|\varrho_{xy}^2/\varrho_{xx}^2$. Note that for the entire illustrations of this study, $B_{xy} = B_{yx} = 0.4$, and for Fig. 1 in particular $\varrho_{qr} = [\varrho_{xx}\ \varrho_{xy}\ \varrho_{yx}\ \varrho_{yy}] = [2\ 1\ 1\ 2]$ mm, these analytically deduced results are almost in exact conformity with the numerical values displayed by the degree of

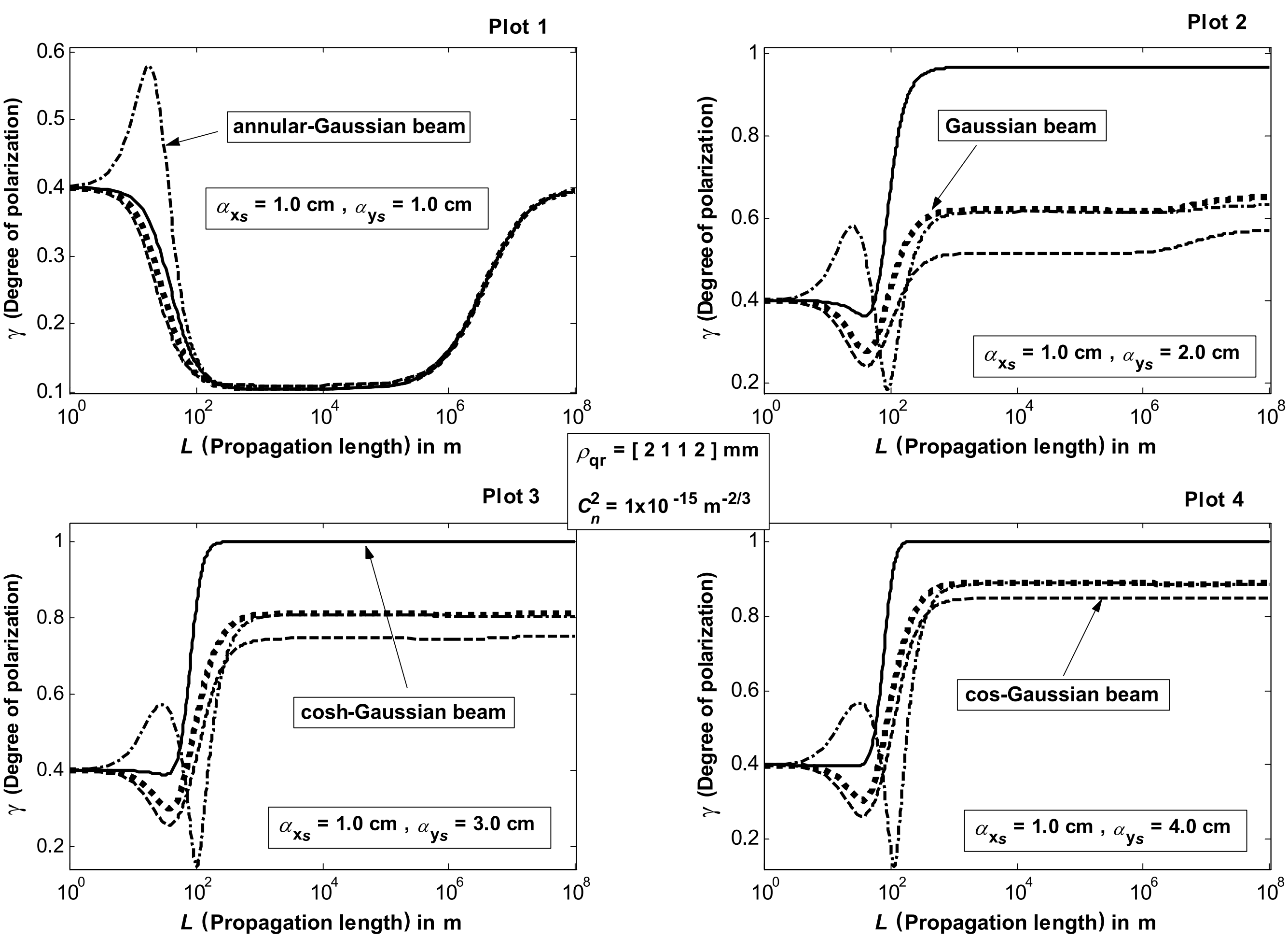

FIGURE 2 Variation of degree of polarization versus propagation length at different source sizes of y polarized beams

polarizations curves in Fig. 1. The unaccounted situations are cosh-Gaussian beam of unequal displacement parameters and the humps of cosh-Gaussian and annular-Gaussian beams.

Now we continue our investigations by plotting in Fig. 2, the degree of polarization for the four beams against propagation path at different source sizes. In this context, the curves in plot 1 of Fig. 2 reflect the typical patterns of Fig. 1, where in both cases, the source sizes of x and y polarized beams are taken equal. From plot 1 of Fig. 2, it is also possible to conclude that, at this source size setting of 1 cm and the displacement parameters being equal to the inverse of the source sizes, the humpy appearance of cosh-Gaussian beam will be removed, but it will continue to exist for annular-Gaussian beam for all individual plots of Fig. 2. Plots 2, 3 and 4 of Fig. 2 prove that, as the source size of the y polarized beam is raised, the degree of polarization at greater propagation ranges, will also be raised towards a saturation value of unity, after a dip at earlier propagation distances. This process will be the fastest for cosh-Gaussian beam and the slowest for cos-Gaussian beam.

Figure 3 explores the variation of the degree of polarization against the structure constant, C_n^2. Here in plot 1, $C_n^2 \rightarrow 0$, hence this implementation represents free space, i.e. no turbulence case. On inserting into (11) the limits of $C_n^2 \rightarrow 0$, followed by $\varrho_0 \rightarrow \infty$ and $L \rightarrow \infty$ in succession, we see that the degree of polarization will once again reduce to $\gamma(\boldsymbol{p}=0, L) \simeq |B_{\mathrm{xy}}|\varrho_{\mathrm{xy}}^2/\varrho_{\mathrm{xx}}^2$. Considering the numerical settings of the used parameters, the degree of polarization will, in the far propagation range, then approximate towards 0.1. This analytically calculated value is well in conformity with the behaviours observed in plot 1 of Fig. 3. According to plots 2, 3 and 4 of Fig. 3, with stronger turbulence, i.e. with higher values of C_n^2, the degree of polarization will revert to the original level at earlier propagation distances.

Finally we examine the variation of the degree of polarization against the coherence parameters. For this purpose, Fig. 4 displays how the degree of polarization reacts to increasing coherence levels. Looking at plots 1–4 of Fig. 4 sequentially, it is seen that as the source self and cross coherence is raised, the width of the dip that is situated between short and long propagation distances becomes narrower. Correspondingly, the initial and the end regions, where the degree of polarization becomes flat, become wider. Another interesting observation regarding Fig. 4 is that, increasing coherence levels causes the differential changes in the degree of polarization to reduce.

Comparing Fig. 1 and the relevant plots of Figs. 3 and 4, one can easily assess that the typical trend for the degree of polarization in turbulent conditions will be more or less preserved given that the only difference between x and y po-

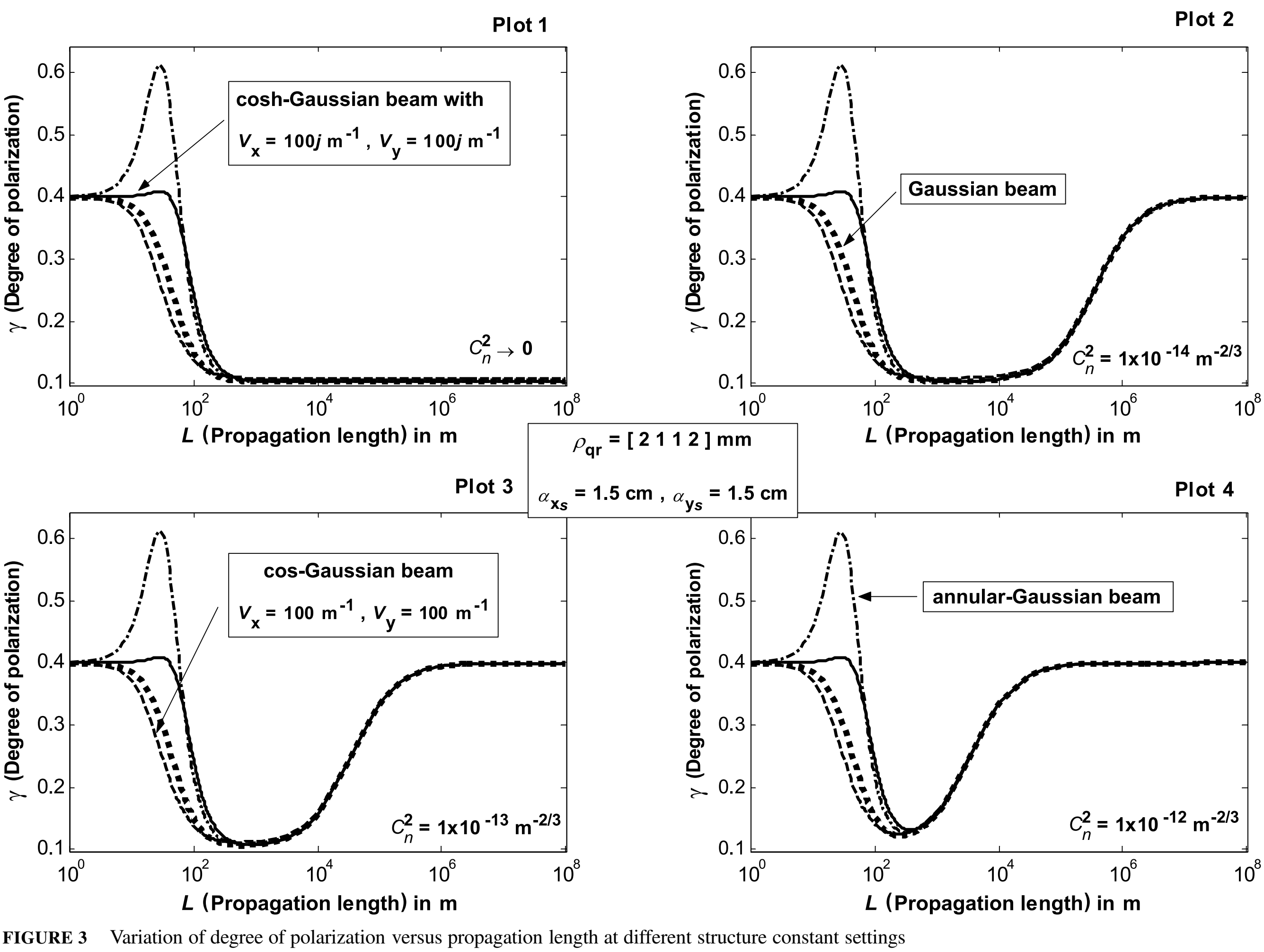

FIGURE 3 Variation of degree of polarization versus propagation length at different structure constant settings

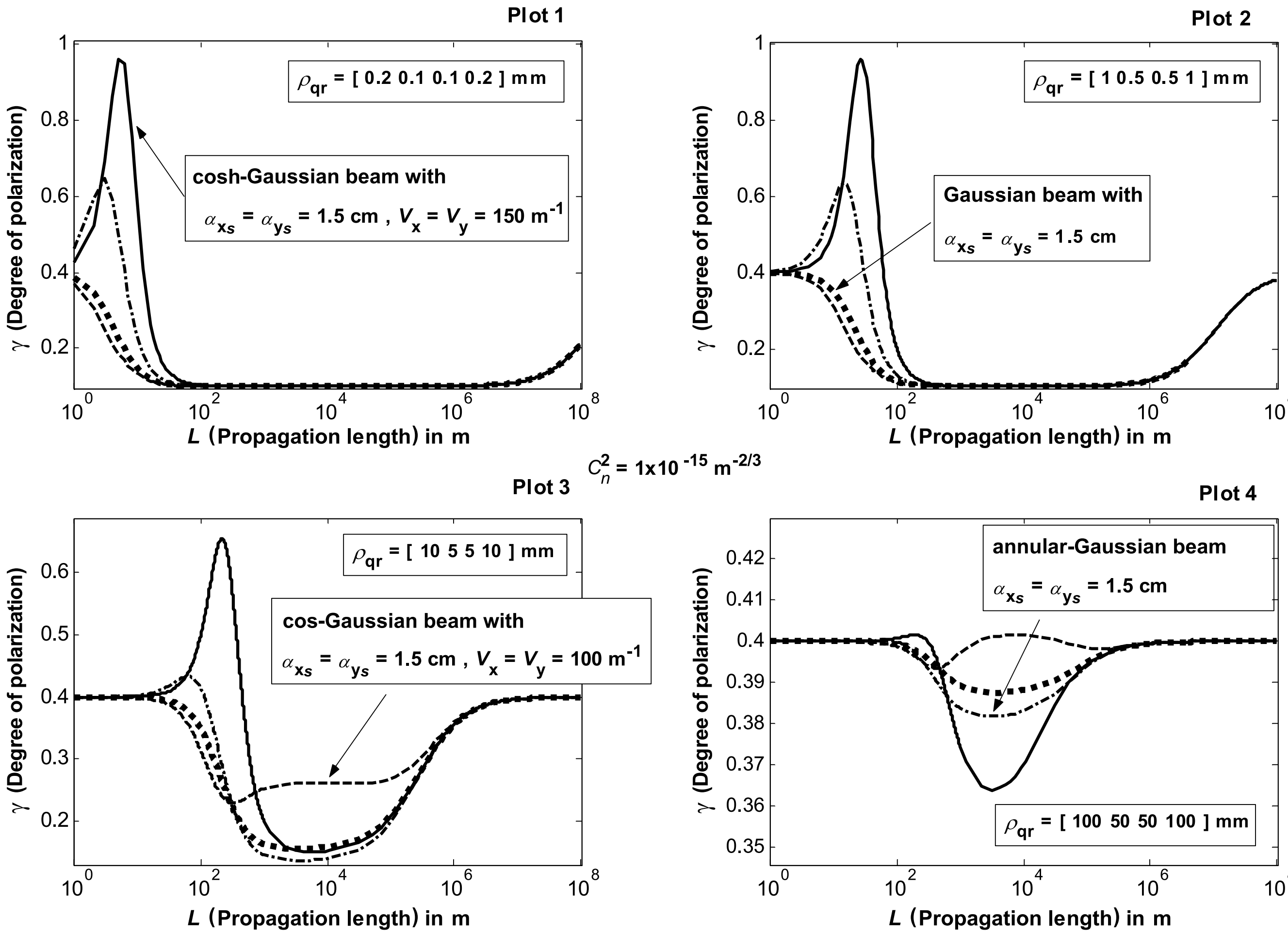

FIGURE 4 Variation of degree of polarization versus propagation length at different degrees of source coherences for self and cross fields

larized fields are the degree of source coherences for self and cross fields.

4 Conclusion

Polarization of cosh-Gaussian, cos-Gaussian and annular-Gaussian optical beams propagating in atmospheric turbulence are investigated. Through the use of mutual coherence functions, the degree of polarization of such beams are evaluated where x and y polarized field components exhibit self and cross partial coherence. For cos-Gaussian beams having equal displacement parameters and for Gaussian beams it is observed that when the degree of partial coherence is the only difference between the x and y polarized source beams, the degree of polarization remains at a constant value for a short propagation distance, while further increase in the propagation length will give rise to a drop in the degree of polarization, and at very long propagation paths, the degree of polarization attains the same value it takes for short propagation lengths. However, for cosh-Gaussian beam with unequal displacement parameters, the behaviour of the degree of polarization versus the propagation length follows an opposite trend. It is found that when the source size of y polarized beam is increased, the degree of polarization at large propagation distances increases and reaches a saturation value of unity, experiencing a dip at smaller propagation distances. Among the beams investigated, this behaviour is the fastest for cosh-Gaussian beams and slowest for cos-Gaussian beams.

Except for the annular-Gaussian beam, the dependence of the degree of polarization on the structure constant is such that in the absence of turbulence, the degree of polarization starts at a certain value and decreases as the propagation length increases, eventually settling at a flat value. As the structure constant is increased, the degree of polarization first stays at a constant value up to a certain propagation distance, decreases as the propagation length increases, forms a dip, then a further increase in the propagation distance yields an increase in the degree of polarization, eventually reaching a saturation value. At higher structure constants, the degree of polarization reverts more rapidly to the saturation value of the smaller propagation distances.

The variation of the degree of polarization versus the propagation distance under different source self and cross coherence shows similar behaviour as in the variation of the degree of polarization versus the propagation distance under different structure constants.

REFERENCES

1 F. Gori, Opt. Lett. **23**, 241 (1998)
2 G. Piquero, F. Gori, P. Romanini, M. Santarsiero, R. Borghi, A. Mondello, Opt. Commun. **208**, 9 (2002)
3 D. Deng, L. Wu, X. Yang, J. Opt. Soc. Am. B **24**, 636 (2007)

4 K. Duan, B. Lü, Opt. Lett. **30**, 308 (2005)
5 F. Gori, M. Santarsiero, G. Piquero, R. Borghi, A. Mondello, R. Simon, J. Opt. A Pure Appl. Opt. **3**, 1 (2001)
6 Y. Cai, D. Ge, Q. Lin, J. Opt. A Pure Appl. Opt. **5**, 453 (2003)
7 G.P. Agrawal, E. Wolf, J. Opt. Soc. Am. A **17**, 2019 (2000)
8 J. Pu, O. Korotkova, E. Wolf, Phys. Rev. E **75**, 056 610 (2007)
9 E. Wolf, Opt. Lett. **28**, 1078 (2003)
10 D. Ge, Y. Cai, Q. Lin, Opt. Commun. **229**, 93 (2004)
11 H. Roychowdhury, S.A. Ponomarenko, E. Wolf, J. Mod. Opt. **52**, 1611 (2005)
12 O. Korotkova, M. Salem, E. Wolf, Opt. Commun. **233**, 225 (2004)
13 X. Ji, E. Zhang, B. Lü, Opt. Commun. **275**, 292 (2007)
14 D.L. Shealy, J.A. Hoffnagle, Appl. Opt. **45**, 5118 (2006)
15 L. Mandel, E. Wolf, *Optical Coherence and Quantum Optics* (Cambridge, Cambridge, 1995)
16 O. Korotkova, Proc. SPIE **61050V**, 1 (2006)
17 Y. Baykal, J. Opt. Soc. Am. A **23**, 889 (2006)
18 H. T. Eyyuboğlu, Y. Baykal, J. Opt. Soc. Am. A **24**, 156 (2007)
19 H. T. Eyyuboğlu, Y. Baykal, Appl. Opt. **46**, 1099 (2007)
20 Y. Baykal, H. T. Eyyuboğlu, Opt. Eng. **45**, 056 001 (2006)
21 I.S. Gradshteyn, I.M. Ryzhik, *Tables of Integrals, Series and Products* (Academic, New York, 2000)
22 Ç. Arpali, C. Yazıcıoğlu, H.T. Eyyuboğlu, S.A. Arpali, Y. Baykal, Opt. Express **14**, 8918 (2006)